Granular Gases under Extreme Driving

W. Kang,[1,*] J. Machta,[1,†] and E. Ben-Naim[2,‡]

[1] *Department of Physics, University of Massachusetts, Amherst, Massachusetts 01003 USA*
[2] *Theoretical Division and Center for Nonlinear Studies, Los Alamos National Laboratory, Los Alamos, New Mexico 87545 USA*

We study inelastic gases in two dimensions using event-driven molecular dynamics simulations. Our focus is the nature of the stationary state attained by rare injection of large amounts of energy to balance the dissipation due to collisions. We find that under such extreme driving, with the injection rate much smaller than the collision rate, the velocity distribution has a power-law high energy tail. The numerically measured exponent characterizing this tail is in excellent agreement with predictions of kinetic theory over a wide range of system parameters. We conclude that driving by rare but powerful energy injection leads to a well-mixed gas and constitutes an alternative mechanism for agitating granular matter. In this distinct nonequilibrium steady-state, energy cascades from large to small scales. Our simulations also show that when the injection rate is comparable with the collision rate, the velocity distribution has a stretched exponential tail.

PACS numbers: 45.70.Mg, 47.70.Nd, 05.40.-a, 81.05.Rm

Granular materials are ubiquitous in nature, but nevertheless, fundamental understanding of the properties of granular materials presents many challenges [1–5]. Underlying these challenges are structural inhomogeneities, macroscopic particle size, and energy dissipation, all of which are defining features of granular matter.

Equilibrium gases have Maxwellian velocity distributions. Due to the irreversible nature of the dissipative collisions, granular gases are out of equilibrium. Indeed, non-Maxwellian velocity distributions are observed in a wide range of experiments in driven granular matter including in particular shaken grains [6–17]. In such experiments, energy is injected *over a wide range of scales* and the measured velocity distribution has a stretched exponential form. To a large extent, a kinetic theory where energy injection through the system boundary is modeled by a thermostat successfully describes these nonequilibrium steady-states [18–21].

Furthermore, theoretical studies suggest that the steady-state is controlled primarily by the ratio between the energy injection rate and the collision rate [22, 23]. When the injection rate is much larger than the collision rate, the velocity distribution is Maxwellian. However, when the injection rate is smaller than the collision rate, the velocity distribution is non-Maxwellian, and has a stretched-exponential tail.

In this study, we focus on the limiting case where the injection rate is vanishingly small and energy is injected at *extremely large velocity scales* [24, 25]. Under such extreme driving, the injected energy cascades down from large velocity scales to small scales and thereby counters the dissipation by collisions. Kinetic theory shows that in the stationary state, the velocity distribution has a power-law high energy tail. These theoretical predictions were supplemented by Monte-Carlo simulations of the homogeneous Boltzmann equation where spatial correlations are ignored. However, such nonequilibrium steady-states have yet to be observed using more realistic molecular dynamics simulations. In this work we carry out extensive molecular dynamics simulations to investigate the behavior of inelastic hard disks under extreme driving.

The goal of this investigation is to establish whether extreme driving is a feasible mechanism for driving granular matter. Our main result is that under rare but powerful injection of energy, a granular gas indeed reaches a stationary state that is characterized by a power-law velocity distribution. Moreover, our simulations quantitatively confirm the predictions of the kinetic theory as the exponent characterizing the tail of the distribution is validated over a wide range of parameters. Our results show that extreme driving is a feasible mechanism for agitating granular matter.

Kinetic Theory. Our starting point is the observation that the purely-collisional homogeneous Boltzmann equation supports stationary solutions [24–27]. The evolution equation for the velocity distribution $f(\mathbf{v})$ of inelastic hard disks takes the form

$$\frac{\partial f(\mathbf{v})}{\partial t} = \iiint d\hat{\mathbf{n}}\, d\mathbf{u}_1\, d\mathbf{u}_2\, |(\mathbf{u}_1 - \mathbf{u}_2)\cdot\hat{\mathbf{n}}|\, f(\mathbf{u}_1) f(\mathbf{u}_2) \times\ [\delta(\mathbf{v}-\mathbf{v}_1) - \delta(\mathbf{v}-\mathbf{u}_1)], \tag{1}$$

with $\hat{\mathbf{n}}$ the impact direction. This Boltzmann equation is supplemented by the inelastic collision rule which specifies the post-collision velocities $\mathbf{v}_{1,2}$ as a linear combination of the pre-collision velocities $\mathbf{u}_{1,2}$,

$$\mathbf{v}_{1,2} = \mathbf{u}_{1,2} - \frac{1+r}{2}(\mathbf{u}_{1,2} - \mathbf{u}_{2,1})\cdot\hat{\mathbf{n}}\,\hat{\mathbf{n}}. \tag{2}$$

In an inelastic collision, the normal component of the relative velocity reverses sign and is scaled

*Electronic address: wfkang@gmail.com
†Electronic address: machta@physics.umass.edu
‡Electronic address: ebn@lanl.gov

down by the restitution coefficient $0 \leq r \leq 1$, $(\mathbf{v}_1 - \mathbf{v}_2)\cdot\hat{\mathbf{n}} = -r(\mathbf{u}_1 - \mathbf{u}_2)\cdot\hat{\mathbf{n}}$. The energy loss equals $\Delta E = -\frac{1-r^2}{4}|(\mathbf{u}_1 - \mathbf{u}_2)\cdot\hat{\mathbf{n}}|^2$.

The collision rule (2) simplifies to a "fragmentation" rule $\mathbf{u} \to (\mathbf{w}_1, \mathbf{w}_2)$ for collisions involving one extremely energetic particle with velocity $\mathbf{u}$ and a second, implicit, particle with speed much less than $|\mathbf{u}|$. The post-collision velocities $\mathbf{w}_1 = \frac{1+r}{2}\mathbf{u}\cdot\hat{\mathbf{n}}\,\hat{\mathbf{n}}$ and $\mathbf{w}_2 = \mathbf{u} - \frac{1+r}{2}\mathbf{u}\cdot\hat{\mathbf{n}}\,\hat{\mathbf{n}}$ follow by substituting $\mathbf{u}_1 = 0$ and $\mathbf{u}_2 = \mathbf{u}$, respectively, into (2). In the limit $|\mathbf{v}| \to \infty$, the nonlinear Boltzmann equation (1) becomes linear and its stationary form is

$$0 = \iint d\hat{\mathbf{n}}\, d\mathbf{u}\, |\mathbf{u}\cdot\hat{\mathbf{n}}|\, f(\mathbf{u})\, [\delta(\mathbf{v}-\mathbf{w}_1) + \delta(\mathbf{v}-\mathbf{w}_2) - \delta(\mathbf{v}-\mathbf{u})]\,. \quad (3)$$

For arbitrary dimension and for arbitrary collision parameters, this linear and homogeneous equation admits the power-law solution

$$f(v) \sim v^{-\sigma}. \quad (4)$$

In two-dimensions, the subject of our investigation, the exponent σ obeys the transcendental equation [24]

$$\frac{1 - {}_2F_1\left(\frac{3-\sigma}{2}, 1, \frac{3}{2}, 1 - (\frac{1-r}{2})^2\right)}{\left(\frac{1+r}{2}\right)^{\sigma-3}} = \frac{\Gamma(\frac{\sigma-1}{2})\Gamma(\frac{3}{2})}{\Gamma(\frac{\sigma}{2})}, \quad (5)$$

where ${}_2F_1$ is the hypergeometric function. The exponent σ grows monotonically with the restitution coefficient. The limiting values are $\sigma = 4.14922$ for completely inelastic collisions ($r = 0$) and $\sigma = 5$ in the elastic limit ($r \to 1$).

The power-law distribution (4) is a stationary solution of the *linear* Boltzmann equation (3). Yet, Monte Carlo methods show that the full *nonlinear* Boltzmann equation (1) does admit a stationary solution with a tail given by (4). These numerical solutions are computed by injecting energy at a rate that is much smaller than the collision rate. In an individual injection event a randomly chosen particle is given a velocity much larger than the typical velocity. Such extreme driving maintains a steady-state in which energy injection balances energy dissipation.

The physical mechanism underlying these driven steady-states is a cascade in which a high energy particle collides with a particle of typical energy yielding two high energy particles, each with energies less than that of the original high energy particle. These two high energy particles produce two more high energy particles, again by collisions with the much more numerous particles with typical energies, and so on.

Scaling Analysis. Interestingly, there is a family of steady-states generated by extreme driving. If $f(v)$ is a stationary solution of (1), then $v_0^{-2} f(v/v_0)$ with the arbitrary typical velocity v_0 is also a stationary solution because the collision rule (2) is invariant under the scale transformation $\mathbf{v} \to \mathbf{v}/v_0$. The energy injection rate γ, the velocity injection scale V, and the typical velocity v_0 are related by the energy balance requirement.

We relate these three quantities by a heuristic argument and first note that the energy injection rate is simply γV^2. Also, we anticipate that the velocity distribution is truncated at the injection scale V. The energy dissipation is dominated by the tail of the distribution and is controlled by the upper cut-off V. We estimate the dissipation rate Γ as follows [28],

$$\Gamma \sim \rho \int^V v \cdot v^2 \frac{1}{v_0^2} f\left(\frac{v}{v_0}\right) v\, dv \sim \rho V^3 (V/v_0)^{2-\sigma}, \quad (6)$$

where ρ is the particle density. In the integrand, the first term v accounts for the collision rate, and the second term v^2 accounts for the energy dissipation in an inelastic collision. The integration is performed using the velocity distribution (4), and since $\sigma < 5$ the dissipation is indeed dominated by the high velocity tail of the distribution. Balancing energy injection with dissipation we obtain a relationship between the injection rate γ, the injection scale V, and the typical velocity v_0,

$$\gamma \sim \rho\, V (V/v_0)^{2-\sigma}. \quad (7)$$

Since the collision rate is proportional to $\rho\, v_0$, the dimensionless ratio ψ of the injection rate to the collision rate scales as a power of the velocity ratio V/v_0,

$$\psi \sim (V/v_0)^{3-\sigma}. \quad (8)$$

Since $\sigma > 3$, we expect a wide power-law range, $V \gg v_0$, when the injection rate is much smaller than the collision rate, $\psi \ll 1$. There is no lower cutoff on the injection rate ψ, below which power-law is not observed; the smaller is ψ, the broader the power-law range. When ψ is order one, the velocity distribution no longer has a power-law tail, and of course, when $\psi \gg 1$, the velocity distribution should simply mirror the distribution of injected velocities.

Molecular Dynamics Simulations. We used molecular dynamics [29] to simulate inelastic hard disks in a square box with elastic walls. In these event driven simulations, upon impact, the velocities of the colliding particles are updated according to the collision rule (2). Subsequent to each collision, we identify the time and location of the next collision. The particles undergo purely ballistic motion between two successive collisions.

We implemented the following velocity-dependent restitution coefficient [30]

$$r(\delta_n) = \begin{cases} 1 - (1-r)(\delta_n/v_c)^{3/4} & \delta_n < v_c, \\ r & \delta_n \geq v_c, \end{cases} \quad (9)$$

where $\delta_n = (\mathbf{v_1} - \mathbf{v_2})\cdot\hat{\mathbf{n}}$ is the normal component of the relative velocity. Here, r is the nominal value of the restitution coefficient, valid at large velocities, and v_c is the cutoff velocity, below which collisions become elastic. With this realistic restitution coefficient [31, 32], we avoid inelastic collapse where an infinite number of collisions can occur in a finite time [33]. Typically, we set v_c

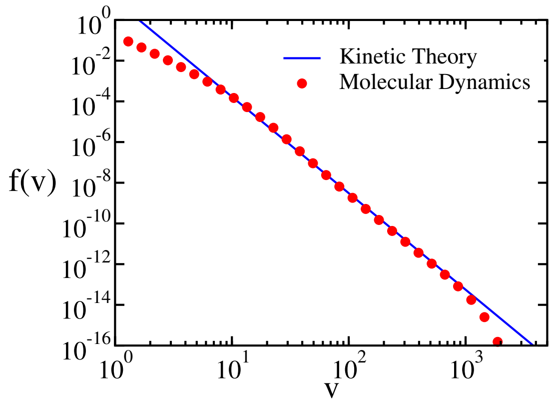

FIG. 1: The velocity distribution $f(v)$ versus the velocity v. Molecular dynamics simulation results (bullets) are compared with the power-law tail predicted by kinetic theory (solid line).

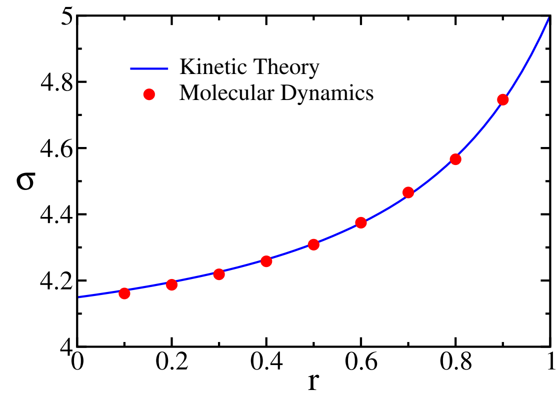

FIG. 2: The exponent σ versus the restitution coefficient r. The molecular dynamics results (bullets) are compared with the kinetic theory predictions (solid line).

much smaller than the typical velocity v_0, but for small restitution coefficients, we must set v_c comparable to v_0 to avoid inelastic collapse.

To maintain a steady-state, we periodically boost a *single* randomly-selected particle to a large, random velocity. These injection events are rare and they are governed by a Poisson process with rate γ, that is, with probability $\gamma\, dt$ injection is implemented during the time interval $[t, t + dt]$. The injection speed is selected from a Gaussian distribution with zero mean and standard deviation V. By taking a long-time average, we confirmed that the total energy approaches a constant, and hence, that the system reaches a statistical steady-state where energy injection and energy dissipation balance. Moreover, the velocity distributions were produced by sampling particle velocities at a very large number (10^8) of equally spaced time intervals. We stress that the velocities are sampled at time intervals that are completely uncorrelated with either collision events or injection events. We tested that our sampling produces robust velocity distributions, and that the velocity distribution, representing an average over the entire system, is truly stationary. In particular, the system does not enter the homogeneous cooling state [34] in between the rare injection events.

We performed numerical simulations using a system of $N = 10^3$ identical particles with diameter $2R = 1$ in a square box of size $L = 400$, corresponding to the low area fraction $\phi = N\pi\,(R/L)^2 = 4.9 \times 10^{-3}$. Unless noted otherwise, these parameters are used throughout this study. Energy was injected at rate $\gamma = 5\times10^{-7}$ and the injection scale was $V = 850$. First, we considered weakly-inelastic particles, $r = 0.9$, with the cutoff $v_c = 0.1$. With these parameters, the injection rate is much smaller than the measured collision rate and their ratio is $\psi = 1.5 \times 10^{-5}$. Consequently, there is substantial scale separation between the typical velocity v_0 and the injection velocity V. Over this range, the steady-state velocity distribution obtained by the molecular dynamics simulations has a power-law high energy tail as in (4) and the exponent $\sigma = 4.74$ is in very good agreement with the kinetic theory prediction given by (5), $\sigma = 4.74104$ (see figure 1). We also confirmed that the ratio $V/v_0 \approx 10^2$ is consistent with the scaling estimate (8).

Next, we varied the restitution coefficient and repeated the simulations. Over the entire parameter range $0.1 \le r \le 0.9$, we find stationary velocity distributions with a power-law tail. In general, the ratio V/v_0 is consistent with the scaling relation (8). Moreover, the exponent σ obtained from the molecular dynamics simulations is in excellent agreement with the kinetic theory predictions (5) for all restitution coefficients (figure 2). We thus arrive at our main result that at least for dilute gases, extreme driving in the form of rare but powerful energy injection generates a steady-state with a broad distribution of velocities. The tail of the velocity distribution is power-law and the characteristic exponent is nonuniversal as it depends on the restitution coefficient.

The fact that kinetic theory holds shows that, to good approximation, the gas is well-mixed. We comment that it is remarkable that extreme driving results in a well-mixed gas. On short time scales, energy injection clearly generates spatial correlations because a just-energized particle transfers much of its energy to nearby particles by inelastic collisions. Yet, on larger time scales energetic particles break coherent structures which are known to be the consequence of inelastic collisions [35]. While these two mechanisms have opposite effects, the simulations indicate that when a long time average is taken, the latter effect dominates. Thus, energy injected at extreme velocity scales in a tightly localized region of space, ends up evenly distributed throughout the system.

Snapshots of the time evolution of the system following energy injection demonstrate how the inelastic cascade works (figure 3). In the initial stages of the cascade, the injection affects only a small region in space and, moreover, there are strong spatial correlations between the velocities of the particles (figure 3 a-c). However, after many inelastic collisions, the injected energy ends up evenly distributed throughout the system (figure 3

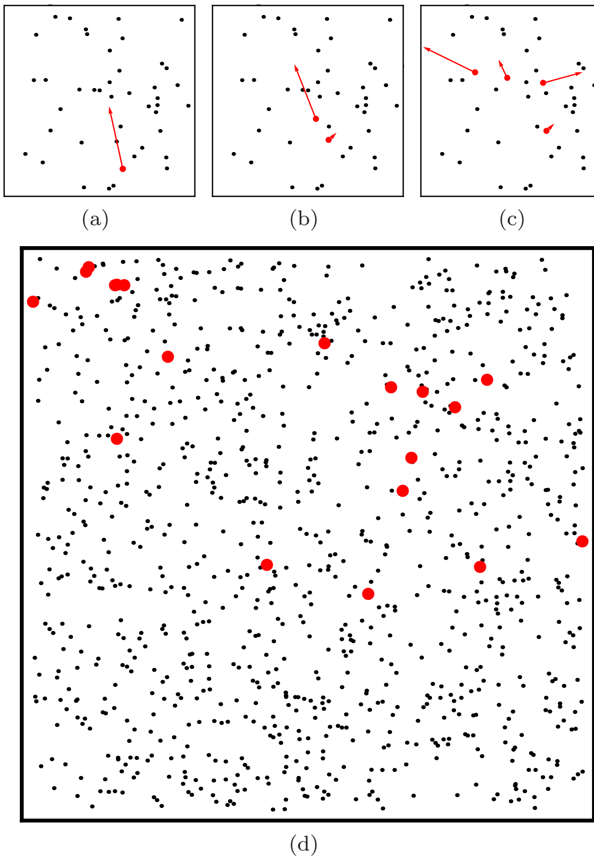

FIG. 3: The inelastic energy cascade. Shown are four time-ordered snapshots of the gas shortly after an injection event. The top three figures show a small window around the injection event in the early stages of the cascade: (a) the initial energetic particle (red online) (b) two energetic particles after one collision, (c) four energetic particles after three collisions. Figure (d) shows the entire system, with energetic particles shown larger (red online), in a late stage of the cascade. After many collisions, the injected energy is evenly distributed throughout the system. The simulation parameters are $r = 0.8$, $N = 1000$, $L = 400$, $V = 707$ and $\gamma = 2 \times 10^{-6}$.

d). When a long time average is taken over many energy injection events at different locations, the system is maintained in a homogeneous, well-mixed state. Spatial correlations induced by inelasticity and the injection mechanism do not affect the predicted power-law velocity distributions.

Therefore, rare, powerful, and spatially localized energy injection is a unique mechanism of agitating granular gases. This mechanism induces an extended energy cascade which distributes the injected energy to the rest of the system. This physical mechanism is different than energy injection by walls [7, 8] or by an effective thermostat [20] or by multiplicative driving [9] where the injected energy directly affects only a small region of space. In this sense, the energy cascade represents a novel mechanism for agitating granular matter.

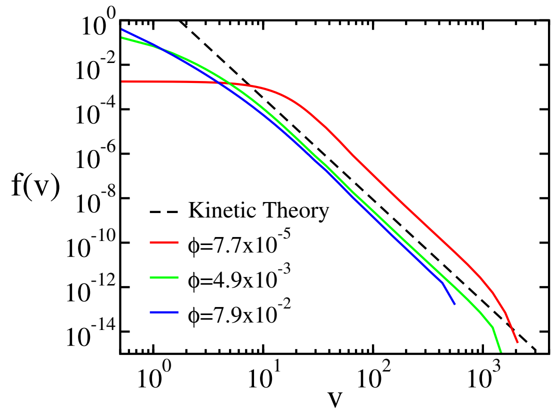

FIG. 4: The velocity distribution at three different densities (solid lines). The simulation parameters are: $r = 0.8$, $\gamma = 2 \times 10^{-6}$, and $V = 707$. Eq. (4) with $\sigma = 4.57246$ is also shown as a reference (dashed line). A best fit to a power-law yields $\sigma = 4.6$, 4.6, and 4.7 for $\phi = 7.7 \times 10^{-5}$, 4.9×10^{-3}, and 7.9×10^{-2}, respectively.

Figure 3 also illustrates that the velocity distribution is correlated with injection times for our system so that the predicted power-law distribution arises only after averaging over many measurements taken at times that are uncorrelated with the injection times. However, for very large systems driven with a fixed but small injection rate per particle there would be many temporally overlapping but spatially well-separated injection events. At any instant of time in a very large system cascades at all stages of development would be present somewhere in the system and the power law tail would be time-independent.

We performed additional simulations to test whether the results are robust with respect to change of parameters. In particular, we varied the area fraction by fixing the number of particles and varying the system size. The results shown in figure 4 are for three different area fractions: $\phi = 7.7 \times 10^{-5}$, $\phi = 4.9 \times 10^{-3}$, and $\phi = 7.9 \times 10^{-2}$. The corresponding values of ψ are 4.7×10^{-4}, 5.4×10^{-5}, and 3.4×10^{-6}, respectively. Note that in all cases $\psi \ll 1$. We find the same power-law tail in all three cases, and the exponent is in good quantitative agreement with the kinetic theory prediction (figure 4). Thus, the energy cascade mechanism can be realized even at area fractions as high as $\phi \approx 10^{-1}$ and with ψ as small as order 10^{-6}.

We also studied the dependence on the ratio ψ between the injection rate and the collision rate by varying the injection rate γ and the injection velocity V. In accord with (8), we find that the range $[v_0, V]$ of power-law behavior shrinks as ψ increases. As long as ψ is sufficiently small, the distribution has a power-law tail (figure 5). When this ratio becomes sufficiently large, the tail is no longer algebraic and a sharper decay occurs. For $\psi = 5.8 \times 10^{-2}$, we find the stretched exponential tail $f(v_x) \sim \exp\left(-\text{const.} \times |v_x|^\zeta\right)$ with $\zeta = 1.52$ (figure 6). This value is consistent with the theoretical value $\zeta = 3/2$ for inelastic gases driven by white noise [20, 21] and the

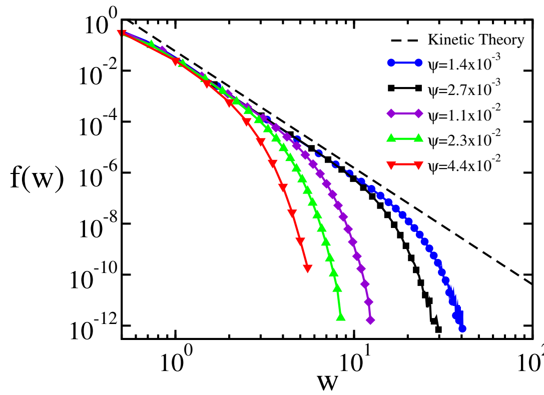

FIG. 5: The velocity distribution $f(w)$ versus the normalized velocity variable $w = v/v_0$ with different ratios of injection rate to collision rate: $\psi = 1.4 \times 10^{-3}$ (bullets), 2.7×10^{-3} (squares), 1.1×10^{-2} (diamonds), 2.3×10^{-2} (up-triangles), and 4.4×10^{-2} (down-triangles). The restitution coefficient is $r = 0.8$. Also shown is the reference theoretical curve (4) with $\sigma = 4.57246$ (dashed line).

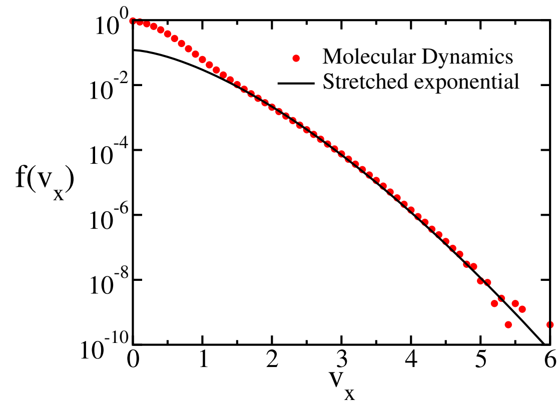

FIG. 6: The distribution $f(v_x)$ of the horizontal component of the velocity v_x at a moderate $\psi = 5.8 \times 10^{-2}$. These simulations are performed with $r = 0.8$, $\gamma = 6 \times 10^{-4}$, and $V = 1.41$. The solid line is a best-fit to the stretched exponential $f(v_x) \sim \exp\left(-\text{const.} \times |v_x|^\zeta\right)$ with $\zeta = 1.52$.

experimental value observed in vigorously shaken beads [10]. Indeed, in this intermediate injection rate regime, the energy cascade becomes localized, and frequent, small injections are similar to white noise driving. On the other hand, these stretched exponential tails do not relate to those observed in [25] as the system cools down after injection is turned-off. We find stretched exponential tails for the range $10^{-1} \lessapprox \psi \lessapprox 1$. When the injection rate exceeds the collision rate ($\psi \gg 1$) the entire distribution becomes Maxwellian as the velocity distribution simply mirrors the distribution of injected velocities.

Finally, we mention that we even varied the energy injection mechanism itself. In particular, to implement injection strictly at large energy scales, we used an "energy loss counter" to keep track of the total energy dissipated by collisions since the last injection. When the dissipated energy equals a fixed large value, we inject this amount of energy into a single randomly chosen particle [24, 25]. Using this variant of extreme driving to maintain the steady-state, we found similar power-law velocity distributions. From these studies, we conclude that the parameter ψ controls the velocity distribution, and that different energy injection mechanisms lead to a power-law distribution with the very same exponent σ, as long as $\psi \ll 1$.

Conclusions. Extensive event-driven simulations show that under extreme driving in the form of rare but powerful energy injections, an inelastic gas reaches a steady-state with a broad distribution of energies. Such driven steady-states are observed for a wide range of collision parameters, densities, and energy injection rates, as long as the injection rate is much smaller than the collision rate. The velocity distributions have a power-law tail and the characteristic exponent is in good agreement with the kinetic theory predictions. When the ratio between the energy injection rate and the collision rate becomes sufficiently large, the velocity distribution has a much sharper stretched exponential tail.

We conclude that extreme driving where energy is injected only at very large scales presents an alternative mechanism for agitating granular matter and that such driving leads to a fundamentally different steady-state compared with traditional driving where energy is injected over all scales. Realizing this driving in experiments is a challenge because the agitation must be applied only at very large velocities. One possible mechanism is shooting very fast particles into the system. While such a system would involve a growing number of particles, the injection of energetic particles should lead to transfer of energy from large scales to small scales by a cascade of collisions.

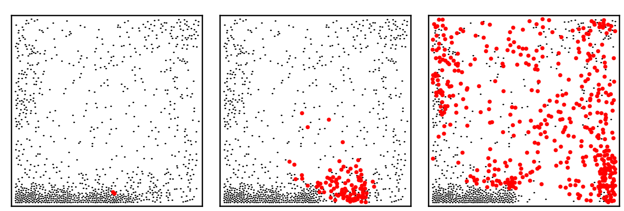

FIG. 7: The time development, left to right, of a cascade in a denser system ($\phi = 7.9 \times 10^{-2}$ and the same parameters as in Fig. 4.) Particles with speeds greater than a fixed threshold are shown larger (red online).

Interestingly, the power-law velocity distribution appears to hold in systems that include dense clusters. We have observed that when the density is increased, there is a tendency for clustering near the walls with no measurable deviation from the predicted power law (figure 7). In this case injection leads to explosive breakup of dense regions. It is intriguing that the power-law tail is quite robust, and extends to situations where the assumptions underlying the kinetic theory approach can no longer be justified.

In our simulations, inelastic collapse does not play a role because collisions become elastic at small relative velocities. Yet, if the collisions are purely inelastic, there should be a competition between the formation of high-density regions by inelastic collisions and the destruction of such clusters by high energy particles. Elucidating this competition is another possibility for further investigation. Nonetheless, our simulations suggest that extreme driving generates well-mixed steady-states despite the fact that this driving is very inhomogeneous in both space and time.

Acknowledgments. We thank Narayanan Menon, Felix Werner for useful discussions and Hong-Qiang Wang for sharing the molecular dynamics code. We acknowledge Financial support from NSF grant DMR-0907235 (JM and WK) and DOE grant DE-AC52-06NA25396 (EB).

[1] H. M. Jaeger, S. R. Nagel and R. P. Behringer, Rev. Mod. Phys. **68**, 1259 (1996).
[2] L. P. Kadanoff Rev. Mod. Phys. **71**, 435 (1999).
[3] P. G. de. Gennes, Rev. Mod. Phys. **71**, S374 (1999).
[4] I. Goldhirsch, Ann. Rev. Fluid. Mech. **35**, 267 (2003).
[5] *Kinetic theory of granular gases*, N. Brilliantov and T. Pöschel, (Oxford, Oxford, 2003).
[6] J. S. Olafsen and J. S. Urbach, Phys. Rev. Lett. **81**, 4369 (1998); Phys. Rev. E **60**, R2468 (1999).
[7] E. L. Grossman, T. Zhou, and E. Ben-Naim, Phys. Rev. E **55**, 4200 (1997).
[8] W. Losert, D. G. W. Cooper, J. Delour, A. Kudrolli and J. P. Gollub, Chaos **9**, 682, 1999.
[9] R. Cafiero, S. Luding, and H. J. Herrmann, Phys. Rev. Lett. **84**, 6014 (2000).
[10] F. Rouyer and N. Menon, Phys. Rev. Lett. **85**, 3676 (2000).
[11] D. L. Blair and A. Kudrolli, Phys. Rev. E **64**, R050301 (2001).
[12] I. S. Aranson, and J. S. Olafson, Phys. Rev. E **66**, 061302 (2002).
[13] K. Kohlstedt, A. Snezhko, M. V. Sakozhnikov, I. S. Aranson, J. S. Olafson, E. Ben-Naim, Phys. Rev. Lett. **95**, 068001 (2005).
[14] A. Prevost and et al, Phys. Rev. Lett. **89**, 084301 (2002).
[15] R. D. Wildman and D. J. Parker, Phys. Rev. Lett. **88**, 064301 (2002).
[16] K. Feitosa and N. Menon, Phys. Rev. Lett. **88**, 198301 (2002).
[17] S. Tatsumi, Y. Murayama, H. Hayakawa, M. Sanoi, J. Fluid Mech. **641**, 521 (2009).
[18] S. E. Esipov and T. Pöschel, J. Stat. Phys. **86**, 1385 (1997).
[19] J. J. Brey and M. J. Ruiz-Montero, Phys. Rev. E **67**, 021307 (2003).
[20] T. P. C. van Noije and M. H. Ernst, Gran. Matt. **1**, 57 (1998).
[21] P. L. Krapivsky, S. Redner, and E. Ben-Naim, *A Kinetic View of Statistical Physics* (Cambridge University Press, Cambridge, 2010).
[22] J. S. van Zon, and F. C. MacKintosh, Phys. Rev. Lett. **93**, 038001 (2004).
[23] J. S. van Zon, and F. C. MacKintosh, Phys. Rev. E **72**, 051301 (2005).
[24] E. Ben-Naim and J. Machta, Phys. Rev. Lett. **94**, 138001 (2005).
[25] E. Ben-Naim, B. Machta, and J. Machta, Phys. Rev. E **72**, 021302 (2005).
[26] M. H. Ernst, E. Trizac, and A. Barrat, Europhys. Lett. **76**, 56 (2006).
[27] E. Ben-Naim and A. Zippelius, J. Stat. Phys. **129** 677 (2007).
[28] Throughout this paper we use the normalization $2\pi\int_0^\infty f(v)\,v\,dv = 1$ where $v \equiv |\mathbf{v}| \equiv \sqrt{v_x^2+v_y^2}$.
[29] B. J. Alder and T. E. Wainwright, J. Chem. Phys. **31**, 459 (1959).
[30] D. Goldman, M. D. Shattuck, C. Bizon, W. D. McCormick, J. B. Swift, and H. L. Swinney, Phys. Rev. E **57**, 4831 (1998).
[31] C. Bizon, M. D. Shattuck, J. B. Swift, W. D. McCormick, and H. L. Swinney, Phys. Rev. Lett. **80**, 57 (1998).
[32] S. Luding, E. Clement, J. Rajchenbach, and J. Duran, Europhys. Lett. **34**, 247 (1996).
[33] S. McNamara and W. R. Young, Phys Fluids A **4**, 496 (1992).
[34] P. K. Haff, J. Fluid. Mech. **134**, 401 (1983).
[35] I. Goldhirsch, and G. Zanetti, Phys. Rev. Lett. **70**, 1619 (1993).